RESEARCH ARTICLE

Advancements in Amorphous Solid Dispersions to Improve Bioavailability

Optimization of Meloxicam Solid Dispersion Formulations for Dissolution Enhancement and Storage Stability Using 3^3 Full Factorial Design Based on Response Surface Methodology

Maha F. Emam[1] · Ahmed A. El-Ashmawy[1] · Nadia M. Mursi[2] · Laila H. Emara[1]

Abstract

This study aimed to formulate and optimize solid-dispersion of meloxicam (MX) employing response-surface-methodology (RSM). RSM allowed identification of the main effects and interactions between studied factors on MX dissolution and acceleration of the optimization process. 3^3 full factorial design with 27 different formulations was proposed. Effects of drug loading percentage (A), carriers' ratio (B), method of preparation (C), and their interactions on percent MX dissolved after 10 and 30 min (Q_{10min} & Q_{30min}) from fresh and stored samples were studied in distilled water. The considered levels were 2.5%, 5.0%, and 7.5% (factor A), three ratios of Soluplus®/Poloxamer-407 (factor B). Physical mixture (PM), fusion method (FM), and hot-melt-extrusion (HME) were considered factor (C). Stability studies were carried out for 3 months under stress conditions. The proposed optimization design was validated by 3-extra checkpoints formulations. The optimized formulation was selected via numerical optimization and investigated by DSC, XRD, PLM, and *in vitro* dissolution study. Results showed that HME technique gave the highest MX dissolution rate compared to other techniques (FM & PM). At constant level of factor (C), the amount of MX dissolved increased by decreasing MX loading and increasing Soluplus in carriers' ratio. Actual responses of the optimized formulation were in close consistency with predicted data. Amorphous form of MX in the optimized formulation was proved by DSC, XRD, and PLM. Selected factors and their levels of the optimization design were significantly valuable for demonstrating and adapting the expected formulation characteristics for rapid dissolution of MX (Q_{10min}= 89.09%) from fresh and stored samples.

Keywords 3^3 full factorial design · hot-melt extrusion (HME) · meloxicam · response surface methodology (RSM) · Soluplus/Poloxamer-407

Introduction

Amorphous solid dispersions (SDs) technique is demonstrably the most simple, efficient, and potent approach for improving the dissolution and bioavailability, particularly for drugs with low solubility (1). SDs are defined as molecular dispersion of poorly water-soluble drugs in inert/biocompatible hydrophilic carrier at solid state (2). Formulation of poorly soluble drugs by SDs is a strategy to tackle dissolution-rate-limited oral absorption that leads to reduction of particle size, enhanced wettability, decreased agglomeration, high porosity, changeability in the physical state, and/or possibly homogenous dispersion of the drug (3). Until now, only a few amorphous products are commercially available, demonstrating inherent problems of their efficacy or the physical instability during shelf-life (4).

Several techniques of SDs have been developed such as solvent-based methods like spray drying (5), solvent evaporation (6), freeze-drying (7), or melt-based methods (fusion and hot melt extrusion "HME" (8). The major problem of

✉ Maha F. Emam
mahafemam@gmail.com

1 Industrial Pharmacy Laboratory, Medicinal and Pharmaceutical Chemistry Department, Pharmaceutical and Drug Industries Research Institute, National Research Centre (Affiliation ID: 10014618), 33 EL Bohouth St. (former EL Tahrir St.), Dokki, P.O.12622, Giza, Egypt

2 Department of Pharmaceutics, Faculty of Pharmacy, Cairo University, Cairo 11562, Egypt

solvent-based methods is the difficulty in the selection of a common volatile solvent and the need for an extra drying step. Also, the yield is always low consequently the scale-up production can be challenging. Accordingly, the preparation of SDs by solvent methods is limited for laboratory studies. While at a larger scale, higher cost of preparation, environmental considerations, and the existence of solvent residuals in the finished product could not be avoided (9).

HME is a process of high shearing and mixing various substances using screw elements at an elevated temperature where the drug and carrier(s) are intimately mixed and melted at a high shearing rate (10). Unlike fusion, the mechanical energy used in HME together with the short heating time will not cause any significant decomposition for most drugs (11).

The flexibility of HME for manufacturing different drug delivery systems is a favorable technology that altered the whole outline of pharmaceutical industrial technology (12). HME is a universally viable alternative to solvent-based techniques. This is the only dust- and solvent-free technology for manufacturing of SDs on a larger scale (13, 14). Moreover, HME is a fast processing, high degree of automation, and continuous operation that makes the scale-up easier (15, 16). Therefore, HME could be considered a cost-effective method for drug development and production (17).

HME technology is still in its nascent stage with a few products commercialized in the market. This could be related to difficulty in manufacture, optimization of variables, and stability concerns associated with such products (18, 19). Formulation of innovative blends of the known approved carriers with plasticizers, surfactants (20), and/or a novel synthetic carrier, in addition to the above-mentioned progress obstacles, to reach the market is the major concern of modern research (21, 22).

Accordingly, the present study investigates the potentiality of applying a novel combination ratio of a new carrier with plasticizer to produce HME of meloxicam (MX) compared to other conventional methods for the first time. The enhancement of MX solubility and correspondingly the dissolution through the formation of SDs with various hydrophilic excipients are widely reported in the literature (23–25). However, a few reports are traced for formulation and stability of SDs of MX using the HME technique due to its excessive degradation and high melting point (26, 27).

MX is a potent selective COX-II inhibitor (NSAID) so, it is safe for the gastrointestinal tract (28, 29). MX has low aqueous solubility (belonging to BCS Class II) which exhibits a slow oral absorption with delayed onset of action, causing failure to give the expected analgesic effect in the desired time (29). It is well-known that MX is nearly totally absorbed after oral administration; however, its absorption rate is distinctly slow with a T_{max} value greater than 5 h (30). There is a direct relation between oral absorption and the gastric emptying rate (GER) of MX because of its incomplete dissolution in the stomach (29). Dissolution studies of MX products are carried out at pH 7.4, while its dissolution at pH 6.4 is much lower, which might be one of the reasons for late MX absorption ($T_{max} > 5h$).

Soluplus® (SOL) is a graft copolymer consisting of polyvinyl caprolactam–polyvinyl acetate–polyethylene glycol. It is proposed as one of the newly used carriers for the design and development of SDs. SOL, compared to traditional solubilizers, has a dual action characteristic, utilized as a matrix carrier for SDs and a solubilizer through micelles formation in an aqueous medium. In addition, SOL acts as self-plasticizers with a suitable Tg (70°C) which allows extrusion at low temperatures and maintains sufficient rigidness for adequate storage stability of the SDs (31). Previous studies reported that extrusion of MX with SOL was processed at relatively high temperatures which resulted in pronounced MX degradation (32). Taha *et al.* (33) successfully developed a novel combination of Soluplus/Poloxamer solid dispersion employing HME, which provided a promising approach for rapid onset of action (*in vivo*) compared to the innovator product (33).

Design of experiments (DoE) is an organized method by which different process parameters are systematically assorted within predetermined ranges; therefore, their effects on the response can be assessed and tested for significance (16). The judicious selection of carriers, drug loading percentage, and manufacturing methods for SD formulations have an ultimate impact on dissolution characteristics and drug stability in the solid-state and *in vivo* performance (2). The effects of different drug loading percentages, manufacturing methods, and carrier(s) on the preparation of MX-SDs could be predicted statistically by response surface methodology (RSM). RSM is strictly related to DOE. RSM is considered a powerful alternative method to solve problems by applying statistical modeling to optimize drug formulation. It is a reliable statistical technique and a critical tool to expect the relation between the independent variables and responses. After statistical calculation of the regression model from suitable experimental data, RSM is effective in optimizing the response function and predicting potential responses (34). By using RSM, the optimized MX formulae can be predicted depending on the fit of the equation to the obtained experimental data of numerous variables that affected the response(s) (35, 36). Furthermore, the multivariate approach of RSM can evaluate the complex interactions of numerous influencing factors and promotes statistical interpretation possibilities (37).

The full factorial design is the most efficient way to investigate a series of intervention components by estimating the main effects from the average of the other effects with a greater prediction ability among models (38). However,

the geometric growth of their samples might be a challenge when additional variables are added.

The objective of the present study was to optimize the formulation of SD with the enhanced dissolution of MX in distilled water employing RSM. The effect of manufacturing methods (HME, fusion, and physical mixtures), drug loading, and carriers' ratio (SOL/POLX) as well as the effect of storage (stability) on product characteristics using a 3^3 factorial design will be studied. The independent variables were the drug loading percentage (A), mixed carriers' ratio (SOL/POLX; B), and the SD preparation techniques (C). The dependent (response) variables investigated were the percent of MX dissolved from both fresh samples in 10 min (Q_{10min}-fresh; Y_1) as well as in 30 min (Q_{30min}-fresh; Y_2), and stored samples in 10 min (Q_{10min}-stored; Y_3) as well as in 30 min (Q_{30min}-stored; Y_4) of MX-SD formulations.

Materials

Meloxicam (MX) powder was kindly provided by Delta-Pharma (Egypt). Soluplus® copolymer (SOL) (Mwt = 118,000 g/mol, density = 1.08 g/cm3) and Poloxamer-407 (POLX) were kindly supplied by BASF-Chemical Company (Ludwigshafen, Germany). Polyethylene glycol 6000 (PEG 6000) was provided by Sigma-Aldrich (USA). Purified water (Millipore-Corporation, USA) was utilized for the preparation of MX release media. Other used chemicals were of analytical grade and were bought from Fisher Scientific.

Methods

Preliminary Studies

Screening of Mixed Carriers

Physical mixtures (PMs) of MX (5% w/w) with two different mixed carriers (SOL/PEG6000 and SOL/POLX), each in a ratio of (50–50), were carefully mixed by trituration in a mortar for 5 min. The prepared PMs were screened through #60 and #45 mesh US standards to get a particle size range of (250–355 μm) and then stored in labeled glass vials until required.

Screening of Particle Size

PM of MX (5% w/w) with SOL/POLX matrix system (in a ratio of 50:50) was screened through #60 and #45 mesh US standards to get two specified particle size ranges (< 250 μm) and (250–355 μm) and then stored in glass vials until required.

Experimental Design and Model Development

A 3^3 full factorial design was created using Design-Expert® software (version 8), to optimize the effect of the three formulation factors using four responses (Tables I and II). Table I lists the factors (independent variables) with their coded and actual levels encompassed by the full factorial design. Two numeric continuous factors, drug loading percentage (A) and mixed carriers' ratio (B), were tested at three levels specified as −1, 0, and +1 (Table I). One categorical factor, method of preparation (C), either PMs, FM, or HME, was designated as −1, 0, or +1, respectively (Table I). The following responses (dependent variables) were analyzed: percent drug dissolved from both fresh formulae at 10 min (Q_{10}; Y_1) and 30 min (Q_{30}; Y_2), as well as stored formulae at 10 min (Q_{10}; Y_3) and 30 min (Q_{30}; Y_4) (Table II). According to the design, a total of 27 runs were generated and performed (Table II). A second-order polynomial function was selected to explain to the developed models as follows:

$$Y_{PM,FM,HME} = \beta_0 + \beta_1 A + \beta_2 B + \beta_{11} A^2 + \beta_{22} B^2 + \beta_{12} AB \tag{1}$$

Where:

$Y_{PM, FM, HME}$	Predicted responses for PMs, FM, and HME, respectively, as types of methods of preparation.
β_0	Intercept
β_1, β_2	Linear coefficients
β_{11}, β_{22}	Square coefficient
β_{12}	Interaction coefficient
A, B	Independent quantitative variables

Table I The Factors (Independent Variables) and Their Levels Encompassed by the Full Factorial Design

Variables	Low Level (−1)	Medium Level (0)	High Level (1)
Numeric variable			
A: drug loading percentage	2.5%	5%	7.5%
B: Carriers' ratio (SOL/POLX ratio)	50–50	60–40	80–20
Categoric variable			
C: Method of preparation	PMs	FM	HME

Table II Matrix of the Full Factorial Design and the Responses (Dependent Variables) Obtained for Each Experimental Run

Standard Order	Run	A (Drug loading %)	B (Mixed carriers' ratio)	C (Method of preparation)	Y_1 (Q_{10min}-fresh)	Y_2 (Q_{30min}-fresh)	Y_3 (Q_{10min}-stored)	Y_4 (Q_{30min}-stored)	%Crystallinity	Solubility (µg/ml)	MX %Recovery
6	1	0	1	−1	21.62±1.50	28.76±1.71	18.62±0.75	27.86±1.06	31.93	32.55±1.31	94.24±1.84
8	2	1	0	−1	11.01±1.18	21.99±1.95	12.96±2.07	22.38±2.01	38.72	26.55±2.71	95.51±2.13
23	3	0	0	1	43.53±1.54	53.15±1.31	42.62±1.21	52.60±1.34	20.63	60.83±2.16	99.85±2.72
14	4	0	0	0	24.44±1.30	26.03±1.21	23.69±1.29	25.11±1.26	34.53	30.99±1.72	97.91±2.90
18	5	1	1	0	26.91±0.79	30.10±0.67	24.09±1.10	29.28±1.12	29.31	35.77±1.07	96.10±1.81
3	6	−1	1	−1	30.38±2.03	34.22±1.78	24.91±1.46	34.24±1.61	27.66	36.71±2.27	94.02±0.82
16	7	1	−1	0	15.35±1.52	20.30±1.21	14.52±1.35	19.57±1.04	40.35	23.52±2.30	95.17±1.63
22	8	0	−1	1	34.20±1.41	51.85±1.17	32.97±1.60	50.14±0.90	21.52	57.53±2.08	96.66±1.18
7	9	1	−1	−1	9.85±0.74	18.96±0.81	9.19±0.96	17.17±0.88	42.93	21.32±1.91	94.38±2.41
25	10	1	−1	1	30.99±1.09	39.62±0.95	27.14±0.77	37.30±1.02	26.25	42.68±1.51	94.70±1.13
17	11	1	0	0	21.17±1.91	22.93±1.28	18.89±1.22	21.27±1.15	38.09	27.74±1.60	95.93±2.62
27	12	1	1	1	55.96±1.54	57.84±1.18	55.05±1.33	56.16±0.98	20.06	61.32±1.40	97.89±1.57
15	13	0	1	0	30.54±1.70	38.21±1.31	29.00±1.28	37.02±1.00	26.53	42.63±1.04	95.86±1.66
12	14	−1	1	0	41.02±1.74	44.64±0.86	36.77±1.67	44.70±1.15	24.98	47.99±1.14	97.53±0.79
2	15	−1	0	−1	18.14±0.93	26.73±1.05	16.87±0.89	23.13±0.78	34.85	30.23±1.51	93.62±1.13
4	16	0	−1	−1	9.53±1.21	18.96±0.79	10.18±1.26	17.20±1.21	42.85	21.72±1.38	94.66±1.68
5	17	0	0	−1	17.69±1.17	25.58±1.36	17.39±1.12	24.51±0.87	36.54	28.14±1.94	94.84±1.41
24	18	0	1	1	65.62±1.11	69.98±1.22	65.26±1.61	68.40±1.78	18.18	72.61±0.85	96.70±1.35
20	19	−1	0	1	70.42±1.45	80.43±1.41	68.49±1.04	78.71±1.41	15.38	83.51±1.15	95.93±1.62
13	20	0	−1	0	17.14±1.28	22.96±1.14	15.65±0.98	21.10±1.17	37.51	27.93±1.46	96.89±1.50
11	21	−1	0	−1	28.73±1.21	31.96±0.99	25.36±0.88	28.03±0.81	28.45	36.03±2.37	95.10±1.81
1	22	−1	−1	−1	11.36±1.34	21.67±1.62	10.77±1.26	19.97±0.67	38.67	26.53±1.24	94.02±0.82
19	23	−1	−1	1	55.01±0.86	76.48±1.54	47.19±1.45	71.46±1.78	16.92	80.02±1.11	95.17±1.63
21	24	−1	1	1	88.41±1.15	95.15±1.31	80.13±1.68	94.30±1.27	13.42	97.85±0.94	99.66±1.18
26	25	1	0	1	30.55±1.45	42.27±1.67	27.89±1.54	40.93±1.17	24.19	49.03±1.45	94.38±1.41
10	26	−1	−1	0	22.17±1.42	28.20±1.19	20.55±1.28	26.23±1.25	32.71	31.23±2.61	95.15±0.65
9	27	1	1	−1	17.84±1.61	24.12±1.28	15.24±1.67	22.89±0.79	36.98	28.73±2.54	93.53±0.71

The design space was established based on the criteria of each response and the desirability function. An optimized batch was manufactured from the optimal value in the obtained design space.

Preparation of Different MX Formulae

MX Physical Mixtures (PMs)

PMs of MX/SOL/POLX, in a predetermined ratio, were prepared by trituration for 5 min in a mortar. The prepared PMs were screened through #60 and #45 mesh US standards to get a specified particle size range (250–355 µm) and then stored in labeled glass vials until required.

MX Solid Dispersions (SDs) by Fusion Method (FM)

Preparation of fusion mixtures (FMs) of MX was carried out via melting the accurately weighed amounts of drug and mixed carriers (SOL/POLX) in a hot plate adjusted at a specified temperature (120°C) using a sand bath. The fused mixture was left to cool and stored in a vacuum oven for 24 h to be solidified. The produced mass was pulverized using mortar and pestle, screened through #60 and #45 mesh US standard to get a specified particle size range (250–355 µm), and then stored in labeled glass vials until required.

MX-HME

SDs of MX/SOL/POLX, in a specified ratio, were melt-extruded using a single screw extruder (¼ inch) with a single rod die (Randcastle Microtruder-RC025, USA). The introduced PMs formed a molten mass between screw walls and extruder barrel, in about 1–3 min. The extrusion pressure was 1 bar, and the residence time was about 3–5 min for the extrudate to come out for different samples. The four extruder zones were adjusted at 110, 110, 105, and 105°C for barrel zones 1, 2, 3, and die-zone, respectively. The screw rotation was fixed at 30 rpm. The produced extrudate was collected and left to cool at ambient temperature and then ground. Finally, the extrudate was screened through #60 and #45 mesh US standards to get a specified particle size range (250–355 µm) and then transferred to labeled glass vials and kept for different analyses.

Evaluation of the Prepared MX Formulae

Drug Content

The assay of MX content was quantitatively analyzed by a reported HPLC/UV method (39). The HPLC apparatus consisted of a multi-solvent delivery system controller (Water 600 E) connected by Waters 2487 dual λ UV/

detector and Rheodyne injector P/N 7725i. A reversed-phase C_{18}-Symmetry® column (3.9 cm × 150 mm i.d., 5 µm particle, Waters-Association, USA) was used as the stationary phase protected by the C_{18}-Symmetry® guard pre-column. The composition of the mobile phase was a mixture of acetonitrile/water (50:50 v/v; pH 3 by glacial acetic acid) pumped at a 1 mL/min flow rate. Millennium 32 software was used to analyze the data.

The LLOQ and the HLOQ of the analytical method were 0.005 and 3 µg/mL, respectively. The accuracy of the method ranged from 93.37 to 101.85%, which was measured as the mean percentage recovery. The analytical precision ranged from 0.0216 to 0.0538% and was determined by the percentage relative standard deviation (RSD%) of the peak area ratios.

An equivalent amount of each prepared formula (containing 15-mg MX) was dissolved in 25 mL methanol. The solution was sonicated and filtered through a 0.45 µm filter (Millex, USA). Adequate dilution with the mobile phase was carried out for the produced filtrate followed by analysis at λ_{max} 360 nm. Fifty-microliter sample was injected; 3 replicates of each sample were analyzed.

In Vitro Dissolution Test

In vitro dissolution studies of different prepared formulae (each equivalent to 15 mg MX) were carried out using a USP apparatus II, paddle dissolution tester (AT8-XTEND, Sotax, Switzerland). Dissolution studies were carried out in filtered, degassed 900 mL of distilled water (measured at 37°C ± 0.2°C and was found pH 6.4). The rate of paddle rotation was fixed at 100 rpm. The dissolution analyses were performed in triplicates.

At designated time points, samples were collected, filtered, and replaced by a fresh dissolution medium. Analysis was carried out spectrophotometrically for MX content at 360 nm utilizing UV-spectrophotometer (Beckman-DU650, USA). MX dissolution rate from each prepared sample was studied in distilled water for 60 min. MX% dissolved after 10 min (Y_1:Q_{10min}-fresh) and 30 min (Y_2:Q_{30min}-fresh) were recorded.

Kinetic Analysis of MX *In Vitro* Dissolution Data

Different mathematical models were tested for the best fitting one with the highest regression coefficient (40); describing the dissolution rate of MX from each formula, viz., zero-order kinetic (Equation 2) (41), first-order kinetic (Equation 3) (42, 43), Higuchi square root of time (Equation 4) (42), and Hixson–Crowell cube root (Equation 5) (42, 44).

$$Q_t = k_0.t \tag{2}$$

$$\ln\left(100 - Q_t\right) = \ln 100 - k_1.t \tag{3}$$

$$Q_t = k_H.t^{1/2} \tag{4}$$

$$\left(100 - Q_t\right)^{1/3} = (100)^{1/3} - k_{HC}.t \tag{5}$$

where Q_t is the percentage (%) drug dissolved in time t; k_0, k_1, k_H, and k_{HC} are coefficient dissolution rate constants for each described model.

Solubility Studies

To assess the enhancement in MX solubility when formulated as SDs, solubility measurements were carried out according to the Higuchi-Connors method (45). A specified weight equal to an excess amount of 15 mg MX each of pure drug or SDs was weighed into glass test tubes, and then 10 mL of distilled water was added. Shaking at 25°C and 100 rpm for 48 h in a temp-controlled shaking water bath (USA) then filtration through a 0.45-µm filter (Mellix, USA) was conducted. Spectrophotometric analysis was carried out at λmax 360 nm against distilled water. All solubility tests were performed in triplicates.

Stability Studies

The prepared formulae were stored in closely sealed glass vials and exposed to stressed conditions set at 40°C $\pm$ 0.5°C with 75% relative humidity (RH) for 3 months. MX % dissolved from stored samples after 10 min (Q_{10min}-stored) and 30 min (Q_{30min}-stored) were recorded. Stability studies of the prepared MX formulae, regarding chemical stability by HPLC in addition to drug *in vitro* dissolution characteristics, were conducted.

Characterization of the Optimized MX Formula

DSC, PLM, chemical stability (via HPLC), and drug *in vitro* dissolution studies *in 0.1N HCL (pH=1.2), distilled water, and phosphate buffer pH 7.4* were carried out for characterization of the optimized MX formula for fresh and 3-month stored samples. For comparing the dissolution behavior of the optimized freshly prepared sample with 3-month stored sample, similarity factor (f_2) as proposed by Moore and Flanner was applied (46).

$$f_2 = 50.\log\left\{\left[1 + (1/n)\,\Sigma_t = 1n\left(R_t - T_t\right)2\right] - 0.5.100\right\} \tag{7}$$

where n is the number of data time points collected during the *in vitro* dissolution test, R_t and T_t are the cumulative dissolution percentages dissolved at the selected (n) time points of the fresh and stored samples, respectively. FDA suggests that two dissolution profiles are considered similar if the similarity factor f_2 is between 50 and 100 (47).

Differential Scanning Calorimetry (DSC)

Powdered samples (MX-pure, carrier(s), and the optimized MX formula) were estimated for their thermal behavior by DSC-Q100 TA-Instruments (USA). Five milligram of each sample was immediately weighed into pierced aluminum pans. The heating ramp was in the range of 25–400°C, at the scaling up rate of 10°C/min. Maintenance of nitrogen purge was at 20 mL/min throughout each run of the thermal analysis. Fresh and stored samples were studied for their thermal behavior. The absolute percent crystallinity, $x(t)$, was calculated from

$$x(t) = \left(\Delta H_t / \Delta H_m\right) \tag{7}$$

where ΔH_t is MX melting enthalpy at time t, which is determined as the ratio of melting enthalpy of the sample divided by the composition of MX, and ΔH_m is the melting enthalpy of 100% crystalline MX at the same heating rate.

X-Ray Diffraction (XRD)

X-ray diffraction patterns of MX, carriers, and the optimized formula (OPT) were obtained using Empyrean Diffractometer, UK. Samples were irradiated with monochromatized Cu Kα 9 radiation at a voltage of 45 kV and a current of 30 mA. The samples were scanned over 3°–80° (2θ) with a step size of 0.02° (2θ) and a time constant of 18.87 s/step.

Polarized Light Microscopy (PLM)

Evaluation of the crystallinity of MX was carried out using the CX41-Olympus microscope (Japan). Suspension of MX samples (pure MX and optimized MX formula) in silicone oil was captured as representative PLM images. Several examination conditions were conducted such as differential interference contrast, using slightly uncrossed polarizers.

Results and Discussion

Preliminary Studies

Screening of Mixed Carriers

Figure 1 depicts the dissolution profiles of different MX-PMs samples containing 5% MX and their corresponding DSC thermograms. It was found that MX-based SOL/POLX (50:50) matrix system showed a higher MX dissolution rate (~1.5-fold) than SOL/PEG6000 (50:50) system with Q_{60min} values of 34.15% and 20.88%, respectively (Figure 1a). This might be attributed to the solubilizing effect of the mixed hydrophilic carriers (SOL/POLX) in the diffusion layer closely surrounding MX particles.

In (Figure 1b), DSC thermograms of MX-PMs samples showed a gradual reduction in ΔH values of MX characteristic melting peak from 49.86 to 32.21% and 25.99% for (MX/SOL/PEG6000) and (MX/SOL/POLX), respectively. These results revealed slight drug-carrier interaction, which might be assigned to the dilution effect of the drug by the carriers and/or dispersion of the drug in the mixed carriers.

In a previous study by Taha *et al.*, (11) MX (2.5%w/w)-based SOL/POLX (in a ratio of 70:30) matrix system showed an enhancement of MX dissolution rate (~10-fold) in HCL even by the simple physical blending. Therefore, MX/SOL/POLX system was selected as a promising carrier matrix system for further characterization studies.

Screening of Particle Size

Figure 2 shows the effect of two different particle size ranges (<250 μm & 250–355 μm) on the dissolution rate of MX from the SOL/POLX matrix system. The dissolution profile of MX was directly proportional to the particle size range; the percent of MX dissolved in 60 min (Q_{60}) increases with
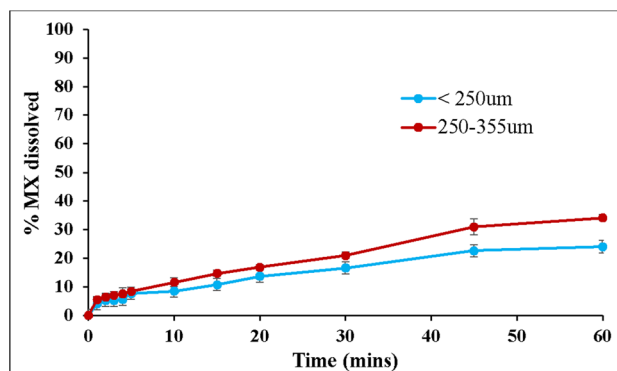
Fig. 2 The effect of particle size on dissolution rate of MX (5% w/w) from SOL/POLX (50:50) matrix system (mean ±SD, $n = 3$)

increasing particle size range (24.00% and 34.15% from < 250 μm and 250–355 μm, respectively). This could potentially be due to smaller particles that might agglomerate and form a cake, resulting in incomplete exposure of the drug substance to the dissolution medium.

Similarly, in previous studies (48, 49), the dissolution of small particles reduced anomalously compared to the larger particles. This result was attributed to the observation that small particles, with poor wettability, had been deposited on the wall and/or agglomerated together resulting in the incomplete dissolution of the drug particles. Therefore, the particle range of 250–355 μm was selected for further optimization design.

Experimental Design

The factors studied (independent variables), such as drug loading %, mixed carriers' ratio, and method of preparation (Table I), were selected based on previous studies (11, 50, 51) for the preparation of different MX/SOL/POLX systems. Table II summarizes the matrix of 3^3 full
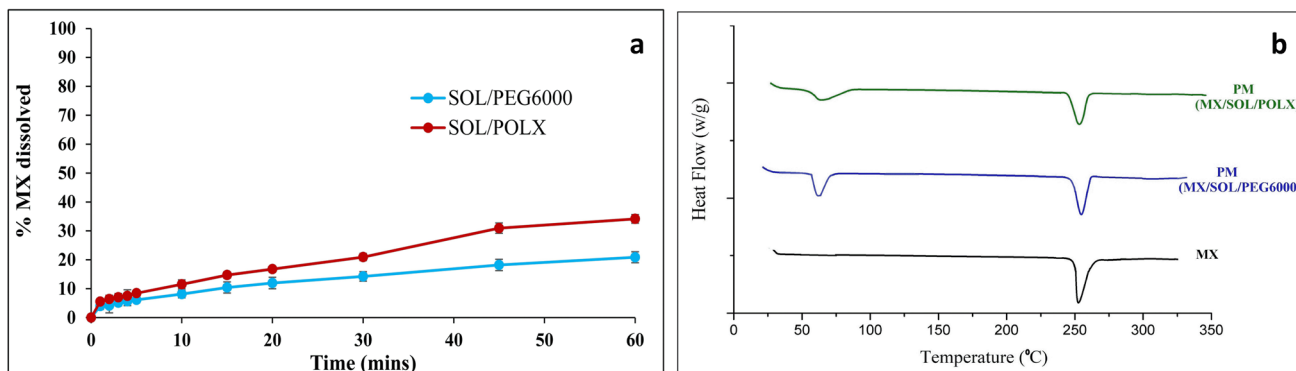
Fig. 1 **a** Dissolution profile of MX (5% w/w) from different PMs samples in a fixed carriers' ratio of (50:50) (mean ±SD, $n = 3$). **b** DSC thermograms of pure MX and PMs of MX/SOL/PEG and MX/SOL/POLX

factorial design, where rows denote the experiments and their achieved responses at the designated levels of the variables investigated in this study. The levels of the studied factors were chosen so that their feasibility and relative differences were suitable to have a quantifiable effect on the response (52).

Model Validation

Analysis of variance (ANOVA) was carried out by Design-Expert® software computer program (version 8) to analyze the effect of each studied factor on individual responses and the adequacy of the suggested model statistically. The sequential model sum of squares was implemented for 2-factor interaction (2FI), linear, cubic, and quadratic models for each response. Design-Expert® computer program recommended a quadratic model as the best fitting of the responses data (Y_1, Y_2, Y_3, and Y_4) based on (i) significant p values resulting from the sum of squares analysis (p values = 0.0106, 0.0350, 0.0233, and 0.0429 for Y_1, Y_2, Y_3, and Y_4, respectively), demonstrating that the model parameters were statistically significant at 95% confidence level; (ii) maximized the adjusted R^2 values (0.9757, 0.9868, 0.9683, and 0.9875 for Y_1, Y_2, Y_3, and Y_4, respectively); and (iii) maximized the predicted R^2 values (0.9573, 0.9753, 0.9381, and 0.9764 for Y_1, Y_2, Y_3, and Y_4, respectively) (38, 53).

Adequate precision of the model, the ratio of signal to noise, and its value > 4 is desirable (54), was also studied. The adequate precisions were 447.87, 280.75, 577.03, and 264.28 for Y_1, Y_2, Y_3, and Y_4, respectively, indicating an adequate signal.

Verification of Model Adequacy

The adequacy of the regression model was also verified between the predicted *versus* actual (experimental data) plots for Y_1–Y_4 as shown in Figure 3. It can be observed that the predicted values came closer to the actual ones and all points on the scatterplot followed a straight line. This implied that the quadratic regression model fitted realistically, thereby adequately expressing the experimental range studied (55).

Drug Content

The drug content percentage of different MX-SDs along with their corresponding PMs is presented in Table II. The mean drug contents were within the range of 93.53 to 99.62% which complied with the accepted pharmacopeial limits (56).

MX *In Vitro* Dissolution Studies

Dissolution testing is essential for the characterization of *in vitro* dissolution data of different IR dosage forms during product development, scaling up, stability studies, and post-approval changes (57). MX dissolution rate from each prepared formula was studied in distilled water for 60 min. For better comparison, the percent drug dissolved up to 10 min (Q_{10min}; fast dissolved stage) and 30 min (Q_{30min}; dissolved stage stated by USP; $Q_{30} \geq 70$ % (58) from fresh and stored samples are chosen for release responses evaluation in the full factorial design.

Q_{10min}-Fresh (Y_1):

Table II reports the percent MX dissolved after 10 min (Y_1) which ranged from 9.53 to 88.41% from various suggested runs. Table III shows that all the main studied factors (A, B & C; p value = <0.0001) and the quadratic terms of numeric factors (A^2 and B^2; p value = 0.0263 and 0.0228, respectively) have significantly influenced the percent of the MX dissolved in 10 min from fresh samples (Y_1). Figure 4 shows a 3-D response surface plot of observed Y_1 caused by changing two independent variables. In each figure, the third factor (method of preparation; C) was kept at a constant level.

Table III and Figure 4 show that drug loading % (A) has a significant effect on Y_1 regression (p-value = <0.0001) with a negative coefficient (−8.48); increasing drug loading % (A) would significantly decrease Y_1. At constant carriers' ratio (B), Y_1 experienced a significant decrease by increasing drug loading % in the predetermined range (Figure 4). When drug loading % was changed from 2.5 to 7.5% at carriers' ratio of (80-20; SOL/POLX), Y_1 was altered from 30.38 to 17.84% (run 6 and 27), from 41.02 to 26.91% (run 14 and 5), and from 88.41 to 55.96% (run 24 and 12) for PMs, FM, and HME, respectively (Table II).

Carriers' ratio (B) exhibited a high magnitude of positive effect (+9.59) in Y_1 regression which was highly significant (p-value = <0.0001) (Table III and Figure 4). In other words, at constant drug loading % (A), Y_1 would significantly increase by increasing SOL in carriers' ratio (B) with upwards curvature in the regression because of the quadratic part of the relationship (Table II and Figure 4). This observation was detected in the entire studied range of drug loading % (2.5%–7.5%). For example, when SOL/POLX ratio was shifted from (50–50) to (80–20) at 2.5% drug loading, Y_1 increased from 11.36% to 30.38% (run 22 and 6), 22.17% to 41.02% (run 26 and 14), and 55.01% to 88.41% (run 23 and 24) for PMs, FM, and HME, respectively (Table II). Therefore, SDs of MX-based SOL/POLX (80-20) matrix system showed the highest dissolution rate followed by SOL/POLX (60–40), and then SOL/POLX (50–50). On the other hand,
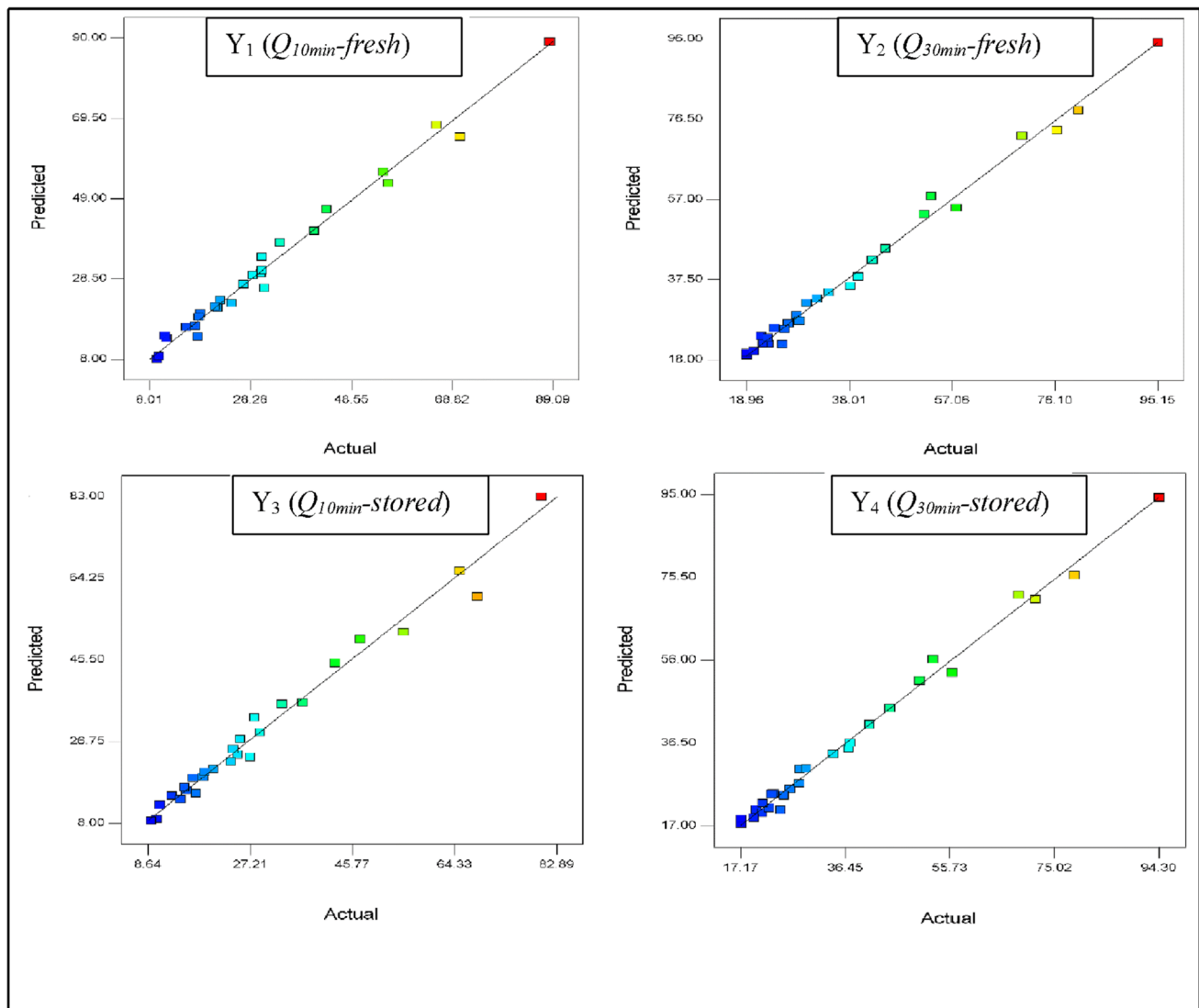
Fig. 3 Predicted *versus* actual plots for Y_1 (Q_{10min}-fresh), Y_2 (Q_{30min}-fresh), Y_3 (Q_{10min}-stored), and Y_4 (Q_{30min}-stored)

the quadratic term of carriers' ratio (*B*) showed a significant negative effect in Y_1 regression (−6.25, *p*-value = 0.0228).

At each level of the categoric variable (C, method of preparation), the maximum % MX dissolved was achieved at the high level of SOL in carriers' ratio (SOL/POLX, 80-20) and low level of drug loading % (2.5%) (Figure 4) where Y_1 was 30.38%, 41.02%, and 88.41% for PM, FM, and HME technique, respectively. Similarly (11), the percent of MX dissolved from SD containing SOL/POLX system in a ratio of (2.3:1.0) was higher than that is containing SOL/POLX (1.5:1.0) matrix system at a 2.5% MX loading ratio.

Regarding the method of preparation (C, categoric factor), HME showed the highest coefficient (+22.49), signifying the highest magnitude on Y_1 compared to FM (−6.73) and PMs (−15.76) (Table III, Figure 4). In other words, HME plays the most significant role in enhancing

MX dissolution among the other studied techniques. At the low level of both A and B, Y_1 was 11.36%, 22.17%, and 55.01% for PM, FM, and HME techniques, respectively. A similar finding was reported by Taha *et al.* (33), where the HME technique gave a higher significant effect on the enhancement of MX dissolution compared to the FM technique.

It was found that AB interaction was not significant (*p*-value = 0.0684), while the interaction of AC and BC variables showed a highly significant effect (*p value*= <0.0001 and 0.0002, respectively; Table III). The interaction of drug loading % with each PM technique and FM technique as well as the interaction of carriers' ratio with HME technique has a positive effect in the Y_1 regression equation. On the other hand, the interaction of drug loading % with the HME technique and the interaction of carriers' ratio with each of

Table III *P*-Value and Estimated Coefficients of the Regression Models for the Studied Responses

	Y_1: Q_{10min}-fresh		Y_2: Q_{30min}-fresh		Y_3: Q_{10min}-stored		Y_4: Q_{30min}-stored	
	p value Prob> F	Coefficient estimate	*p* value Prob> F	Coefficient estimate	*p* value Prob> F	Coefficient estimate	*p* value Prob> F	Coefficient estimate
Model	< 0.0001		< 0.0001		< 0.0001		< 0.0001	
Intercept		36.59		40.66		36.75		39.95
A. Drug loading %	< 0.0001	−8.48	< 0.0001	−9.22	< 0.0001	−7.23	< 0.0001	−8.95
B. Carriers' ratio	< 0.0001	9.59	< 0.0001	6.89	< 0.0001	8.94	< 0.0001	7.48
C. Preparation method	< 0.0001		< 0.0001		< 0.0001		< 0.0001	
AB	0.0684	−1.66	0.0975	−1.14	0.2873	−1.00	0.0103	−1.83
AC	< 0.0001		< 0.0001		< 0.0001		< 0.0001	
BC	0.0002		0.0034		< 0.0001		0.0025	
A^2	0.0263	3.15	0.0183	2.59	0.3238	1.40	0.0339	2.21
B^2	0.0228	−6.25	0.0413	−2.28	0.0099	−7.84	0.1443	−2.82

*Statistically significant: p < 0.05

the PM and FM techniques showed a negative effect in Y_1 regression.

Model reduction through the manual exclusion of insignificant terms for Y_1 was performed. The final empirical equation for estimating Y_1 in terms of coded factors can be expressed by Equations (8, 9, 10):

$$Y_{1PM} = +7.38005 - 5.49222\,A + 20.48552\,B \\ - 0.44171\,AB + 0.50376\,A^2 - 2.77913\,B^2 \tag{8}$$

$$Y_{1FM} = +17.84650 - 5.98042\,A + 20.88772\,B \\ - 0.44171\,AB + 0.50376\,A^2 - 2.77913\,B^2 \tag{9}$$

$$Y_{1HME} = +56.57174 - 10.50330\,A + 26.12879\,B \\ - 0.44171\,AB + 0.50376\,A^2 - 2.77913\,B^2 \tag{10}$$

Where:

Y_{1PM}, Y_{1FM}, Y_{1HME}: Predicted responses for % MX dissolved in 10 min (Q_{10min}; Y_1) from fresh formulae prepared by physical mixture, fusion method, and hot-melt extrusion, respectively

A: Drug loading %

B: Carriers' ratio

AB: Interaction coefficient of drug loading % and carriers' ratio

Q_{30min}-Fresh (Y_2):

Table II shows the percent of MX dissolved after 30 min (Y_2) from fresh formulae which ranged from 18.96 to 95.15% in various suggested runs. All the main studied factors (A, B, and C; *p*-value = <0.0001) and the quadratic terms of numeric factors (A^2 and B^2; *p*-value =0.0183

and 0.0413, respectively) have significantly affected the percent of MX dissolved in 30 min from samples (Y_2) (Table III). 3-D response surface plot of observed Y_2 caused by changing two independent variables, each at a constant level of categoric factor, has been presented graphically in Figure 4.

Table III and Figure 4 show that drug loading % (A) showed a high magnitude of effect (−9.22) in Y_2 regression which was highly significant (*p*-value = <0.0001) with a negative effect. In other words, at constant carriers' ratio (B), Y_2 would significantly increase by decreasing drug loading % (A) with downwards curvature in the regression because of the quadratic part of the relationship (Table II and Figure 4). This was experienced for all three studied carriers' ratios. At constant carriers' ratio (B), increasing drug loading % from 2.5 to 7.5% had caused a considerable decrease in Y_2.

Carriers' ratio (B) showed a significant effect in Y_2 regression with a positive coefficient (6.89, *p*-value = <0.0001; Table III); increasing SOL in carrier's ratio (SOL/POLX) from (50–50) to (80–20) would significantly increase Q_{30min} (Y_2) at constant drug loading % (Figure 4). However, carriers' ratio (B) showed a significant quadratic effect with a small negative coefficient (−2.28, *p*-value= 0.0413).

At each level of the categoric variable (C, method of preparation), the maximum Q_{30min} (Y_2) value was achieved at the low level of drug loading % (2.5%) and high level of SOL in carriers' ratio (SOL: POLX, 80-20) (Figure 4) where Q_{30min} (Y_2) was 34.22%, 44.64%, and 95.15% for PM, FM, and HME technique, respectively.

For all the tested formulae, the method of preparation (C; categoric factor) showed a highly significant effect on Y_2
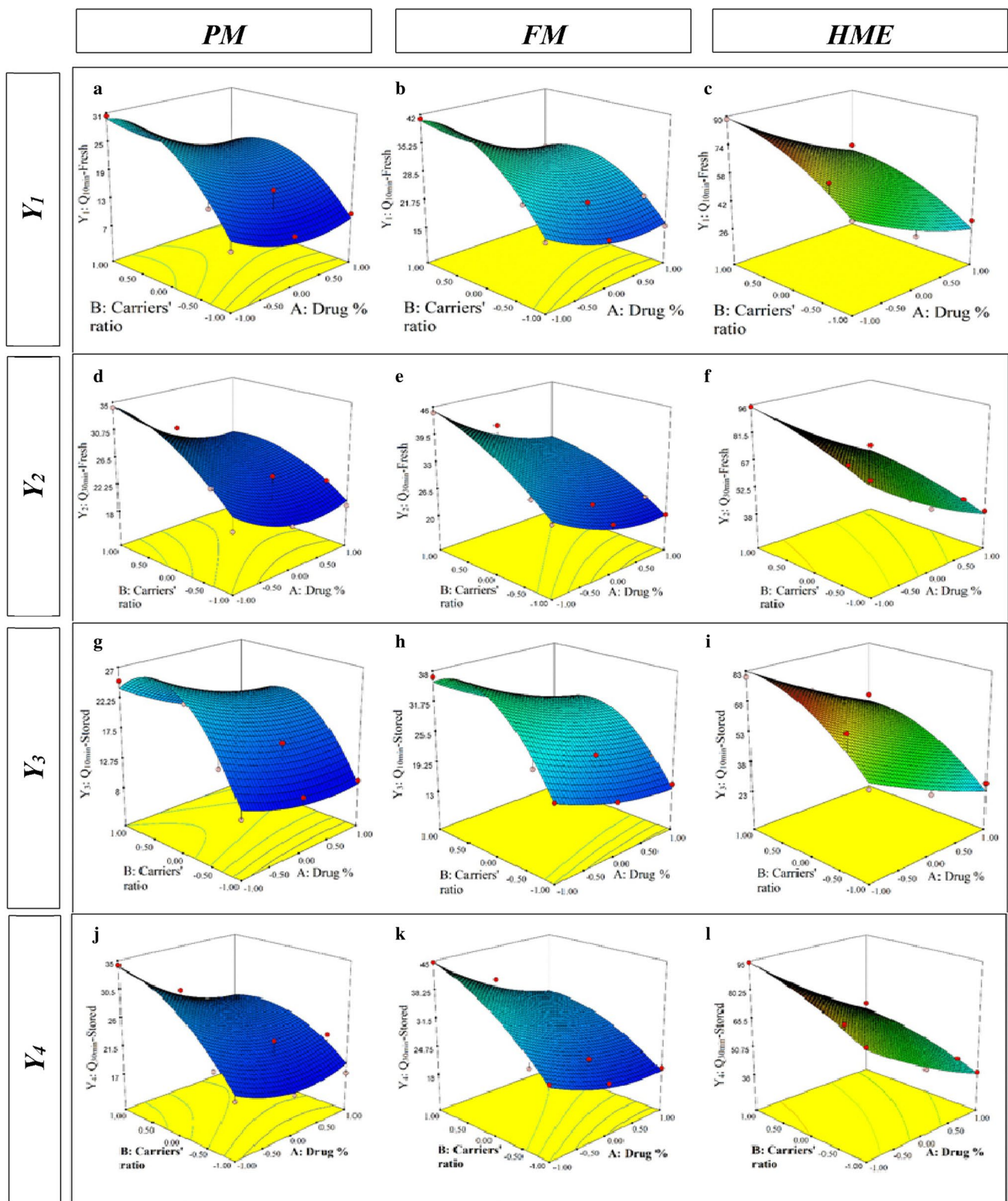
Fig. 4 3-D response surface plots of Y_1-Y_4, each sub-figure represents each method of preparation (PM, FM, and HME)

(p-value = <0.0001; Table III). HME technique showed the highest positive coefficient (24.55) relative to FM (−9.50) and PMs (−15.05) (Table II, Figure 4). At the low level of both A and B, the percent of MX dissolved in 30 min (Y_2) was 21.67%, 28.20%, and 76.48% for PM, FM, and HME techniques, respectively.

AB interaction was not significant (*p*-value = 0.0975), while the interaction of AC and BC variables showed a highly significant effect (*p-value* = <0.0001 and 0.0034, respectively; Table III). The interaction of drug loading % with each of PM and FM techniques as well as the interaction of carriers' ratio with each of FM and HME techniques has a positive coefficient in the Y_2 regression equation, whereas the interaction of drug loading % with HME technique and the interaction of carriers' ratio with PM technique showed a negative effect in the Y_2 regression equation.

Model reduction through the manual exclusion of insignificant terms for Y_2 was performed. The final empirical equation for estimating Y_2 in terms of coded factors can be expressed by Equations (11, 12, 13):

$$Y_{2PM} = +25.24120 - 4.65673A + 9.36748\,B \\ - 0.30456\,AB + 0.41458\,A^2 - 1.01201\,B^2 \tag{11}$$

$$Y_{2FM} = +30.73446 - 5.58410\,A + 11.24682\,B \\ -0.30456\,AB + 0.41458\,A^2 - 1.01201\,B^2 \tag{12}$$

$$Y_{2HME} = +87.56987 - 10.97456\,A + 12.91415\,B \\ -0.30456\,AB + 0.41458\,A^2 - 1.01201\,B^2 \tag{13}$$

Where:

Y_{2PM}, Y_{2FM}, Y_{2HME}: Predicted responses for % MX dissolved in 30 min (Q_{30min}; Y_2) from fresh formulae prepared by PMs, FM, and HME, respectively

A: Drug loading %

B: Carriers' ratio

AB: Interaction coefficient of drug loading % and carriers' ratio

Q_{10min}-Stored (Y_3):

Percent MX dissolved after 10 min (Y_3) from stored formulae for 3 months at 40°C/75%RH which ranged from 9.19 to 80.13% in various suggested runs (Table II). All the main studied factors (A, B, and C; *p*-value = <0.0001) and the quadratic terms of (B^2; *p*-value= 0.0099) have significantly influenced the percent of MX dissolved in 10 min from stored samples (Y_3) (Table III). 3-D response surface plot of observed Y_3 caused by changing two independent variables, at constant of factor (C), has been presented graphically in Figure 4.

Table III and Figure 4 show that drug loading % (A) showed a significant effect in Y_3 regression with a negative coefficient (−7.23, *p-value* = <0.0001); increasing drug loading % (A) would significantly decrease Y_3. At the constant level of (B), Y_3 has experienced a significant decrease by increasing drug loading % in the predetermined range (Figure 4); when drug loading % was changed from 2.5%

and 7.5% at carriers' ratio of (80-20; SOL/POLX), Y_3 was altered from 24.91% to 15.24% (run 3 and 9) and 36.77% to 24.09% (run 12 and 18) from 80.13% to 55.05% (run 21 and 27) for PMs, FM, and HME, respectively (Table II). However, the quadratic term (A^2) was not significant (*p*-value= 0.3238; Table III).

Carriers' ratio (B) showed a highly significant positive effect (8.49, *p*-value = <0.0001) in Y_3 regression (Table III and Figure 4). In other words, at constant drug loading %, Y_3 would significantly increase by increasing SOL in carriers' ratio (B) with upwards curvature in the regression because of the quadratic part of the relationship (Table II and Figure 4). This finding was detected in the entire studied range of drug loading %. While SOL/POLX ratio was shifted from their low levels (50−50) to their high levels (80-20) at constant drug loading % of 2.5%, Y_3 increased from 10.77% to 24.91% (run 1 and 3), 20.55% to 36.77% (run 10 and 12) and 47.19% to 80.13% (run 19 and 21) for PMs, FM and HME, respectively (Table II). Therefore, HME of MX-based SOL/POLX matrix system (in a ratio of 80-20, level 1) showed the highest dissolution rate followed by SOL/POLX (60−40, level 0) then SOL/POLX (50−50, level −1).

At each level of the categoric variable (C, method of preparation), the maximum MX dissolved was achieved at the low level of drug loading % (2.5%) and high level of SOL in carriers' ratio (SOL: POLX; 80-20) (Figure 4) where Y_3 was 24.91%, 36.77%, and 80.13% for PM, FM, and HME technique, respectively.

For all the tested formulae, the method of preparation (C; categoric factor) showed a highly significant effect on Y_3 (*p*-value = <0.0001; Table III). HME technique showed the highest coefficient (+21.75), signifying the dominance of HME for enhancement of MX dissolution rate relative to FM (−6.65) and PMs (−15.10) techniques (Table II, Figure 4). At the low level of both A and B, the percent of MX dissolved from stored samples in 10 min (Y_3) was 10.77%, 20.55%, and 47.19% for PM, FM, and HME techniques, respectively (Table III).

AB interaction was not significant (*p*-value = 0.2873). The interaction of AC and BC variables showed a highly significant effect (*p*-value= <0.0001; Table III) where the interaction of drug loading % with each of PM and FM techniques as well as the interaction of carriers' ratio with HME technique has a positive coefficient in the Y_3 regression equation, whereas the interaction of drug loading % with the HME technique and the interaction of carriers' ratio with each of FM and PM techniques showed a significant negative effect on Y_3 regression.

Model reduction through the manual exclusion of insignificant terms for Y_3 was performed. The final empirical equation for estimating Y_3 in terms of coded factors can be expressed by Equations (14, 15, 16):

$$Y_{3PM} = -0.38616 - 2.67708\,A + 21.96363\,B \\ - 0.26704\,AB + 0.22454\,A^2 - 3.48270\,B^2 \tag{14}$$

$$Y_{3FM} = +8.31842 - 3.34457\,A + 23.19877\,B \\ - 0.26704\,AB + 0.22454\,A^2 - 3.48270\,B^2 \tag{15}$$

$$Y_{3HME} = +42.48555 - 7.38193\,A + 28.96282\,B \\ - 0.26704\,AB + 0.22454\,A^2 - 3.48270\,B^2 \tag{16}$$

Where:

Y_{3PM}, Y_{3FM}, Y_{3HME}: Predicted responses for % MX dissolved from stored samples in 10 min (Q_{10min}-stored) from fresh samples prepared by PMs, FM, and HME, respectively

A: Drug loading %
B: Carriers' ratio
AB: Interaction coefficient of drug loading % and carriers' ratio

Q_{30min}-Stored (Y_4):

Percent MX dissolved after 30 min from stored samples (Y_4) for 3 months at 40°C/75%RH which ranged from 17.17 to 94.30% in various suggested runs (Table II). All the main studied factors (A, B, and C; p-value = <0.0001) and the quadratic terms of (A^2; p-value= 0.0339) have significantly influenced the percent of MX dissolved in 30 min from stored samples (Y_4) (Table III). 3-D response surface plot of observed Y_4 caused by changing two independent variables, each at a constant level of the third categoric factor, has been presented graphically in Figure 4.

Table III and Figure 4 show that drug loading % (A) showed a highly significant negative effect (−8.95, p-value = <0.0001) in Y_4 regression. In other words, at constant carriers' ratio, Y_4 would significantly increase by decreasing drug loading % (A) with downwards curvature in the regression because of the quadratic part of the relationship (Table II and Figure 4). This was experienced for all three studied carriers' ratios. At the constant B level, shifting drug loading % from 2.5 to 7.5% had caused a significant decrease in Y_4.

Carriers' ratio (B) showed a significant effect in Y_4 regression with a positive coefficient (7.48, p-value = <0.0001; Table III); shifting carriers' ratio from their low levels (50−50) to their high levels (80-20) would increase Y_4 at constant drug loading % (Figure 4). However, the quadratic term (B^2) showed a non-significant effect (p-value= 0.1443).

At each level of the categoric variable (C, method of preparation), the maximum Y_4 was achieved at the low level of drug loading % (2.5%) and high level of SOL in carriers' ratio (SOL: POLX; 80-20) (Figure 4) where Y_4

was 34.24%, 44.70%, and 94.30% for PM, FM, and HME technique, respectively.

For all the tested formulae, the method of preparation (C; categoric factor) showed a highly significant effect on Y_4 (p-value = <0.0001; Table III). HME technique showed the highest positive coefficient (+24.22), signifying the dominance of HME for enhancement of MX dissolution rate relative to FM (−9.40) and PMs (−14.82) techniques (Table III, Figure 4). At the low level of both A and B, Y_4 was 19.97%, 26.23%, and 71.46% for PM, FM, and HME techniques, respectively.

AB interaction showed a significant negative effect (−1.83, p-value = 0.0103; Table III); decline in Y_4-value when both A and B were in their high or low levels. Moreover, the interaction of AC and BC variables showed a highly significant effect (p-value= <0.0001 and 0.0025, respectively; Table III) where the interaction of drug loading % with each of PM and FM techniques and the interaction of carriers' ratio with each of FM technique and HME technique have a positive coefficient in the Y_4 regression equation, whereas the interaction of drug loading % with HME technique and the interaction of carriers' ratio with PM technique showed a negative effect in Y_4 regression.

Model reduction through the manual exclusion of insignificant terms for Y_4 was performed. The final empirical equation for estimating Y_4 in terms of coded factors can be expressed by Equations (17, 18, 19):

$$Y_{4PM} = +17.94428 - 3.47336\,A + 11.85527\,B \\ - 0.48920\,AB + 0.35401\,A^2 - 1.25138\,B^2 \tag{17}$$

$$Y_{4FM} = +23.15854 - 4.40303\,A + 13.79732\,B \\ - 0.48920\,AB + 0.35401\,A^2 - 1.25138\,B^2 \tag{18}$$

$$Y_{4HME} = +79.79305 - 9.81887\,A + 15.42260\,B \\ - 0.48920\,AB + 0.35401\,A^2 - 1.25138\,B^2 \tag{19}$$

Where:

Y_{4PM}, Y_{4FM}, Y_{4HME}: Predicted responses for % MX dissolved from stored samples in 30 min (Q_{30min}-stored) from fresh samples prepared by PMs, FM and HME, respectively

A: Drug loading %
B: Carriers' ratio
AB: Interaction coefficient of drug loading % and carriers' ratio

These results revealed that MX dissolution rate in 10 and 30 min from different freshly (Y_1 & Y_2) and stored (Y_3 & Y_4) formulae in distilled water were negatively affected by drug loading % (A) (Figures 5I). Increasing drug loading % from 2.5 to 7.5% would slow down % MX dissolved, this counterintuitive result can be explained by increasing the observed rigidity and stiffness of the

prepared SD during the HME process with increasing concentration of a high melting point drug (MX melting temp = 255°C). Similarly, Serajuddin *et al.* (59) reported that the dissolution rate of carvedilol SD with Kollidon® VA64 prepared by the HME technique decreased with increasing drug loading percentage from 5 and 10% to 20% w/w drug. On the other hand, (Y$_1$-Y$_4$) were positively affected by the carriers' ratio, and the highest dissolution rate was observed at a high ratio of SOL in the mixed carriers' system (80−20, level 1) (Figure 5II). This could be attributed to the increasingly solubilizing effect with a high ratio of SOL in the diffusion layer directly surrounding drug particles.

It is worth mentioning that all HME formulae exhibited an enhanced dissolution rate compared to other techniques (FM and PM) (Figure 5III). This emphasized the superiority of HME to provide the most intimate dispersion of MX in the carrier(s) matrices and facilitate its transfer to the amorphous form with magnificent improvement in its dissolution (12, 60).

On the other hand, a study by Hughey *et al.* (32) reported that HME was not a viable technique for amorphous

dispersion of MX/SOL as it required high processing temperatures of 175°C and yielded only 88% potency.

Previously, an attempt to extrude MX-based SOL pellets by HME with enhanced dissolution and bioavailability (in human subjects) was successful (51) . Additionally, the introduction of a novel carrier combination of SOL/POLX facilitates the extrusion of MX at lower temperatures and helps to alleviate current limitations imposed by drug-carrier matrix incompatibilities (33).

Kinetic Analysis of the *In Vitro* Dissolution Data of MX:

The results of regression analysis of MX dissolution data from different prepared formulae before and after storage were summarized in Supplementary Tables I and II. Twenty-four out of twenty-seven fresh formulae followed the Higuchi square root of time model as denoted by the highest regression coefficient (r^2) (Supplementary Table I). This model is dependent on Fickian diffusion, which illustrates a direct correlation of the square root of time with drug release from an insoluble matrix (40). In addition, three formulae followed the Hixson–Crowell cube root model that
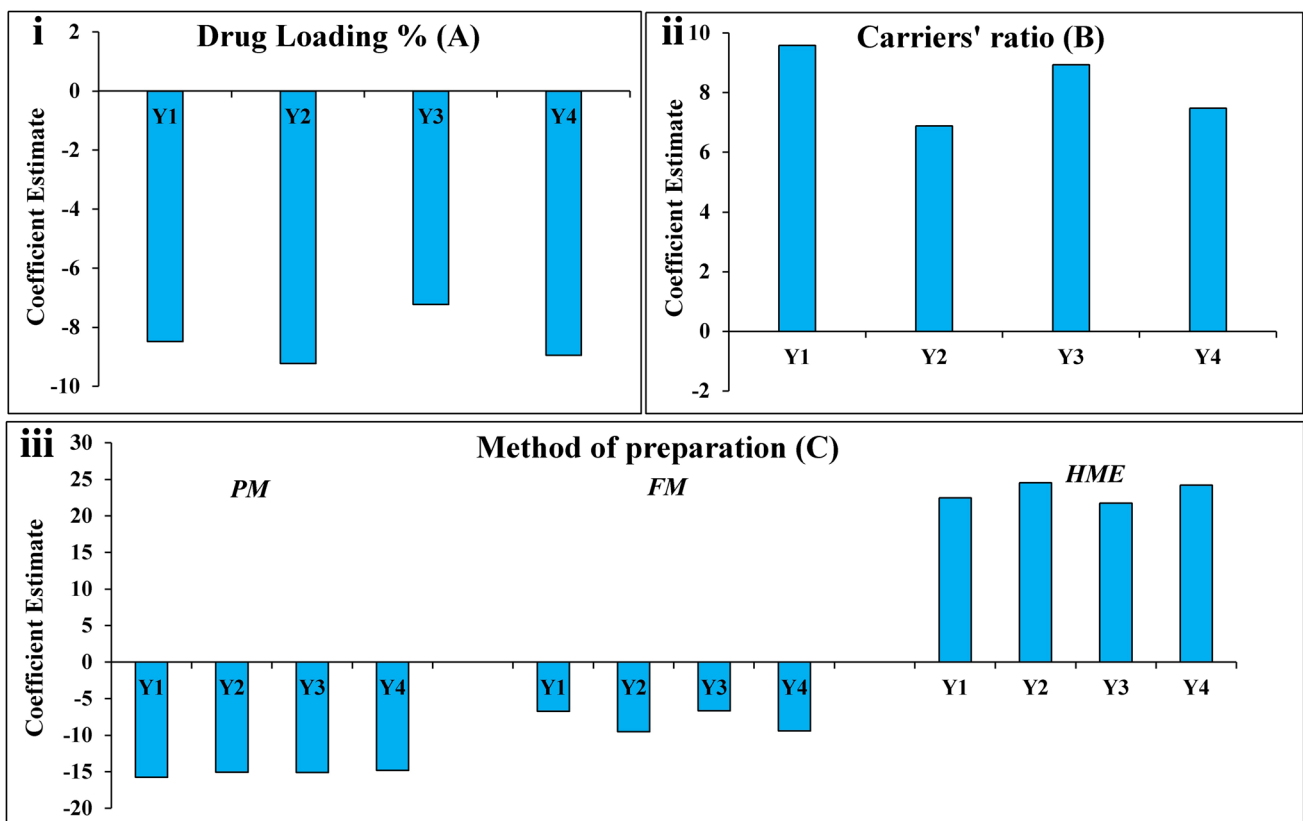

Fig. 5 Coefficient estimates of the studied factors for each response

characterizes the release of the drug to rely on the change in the particles' diameter and surface area with time. It primarily applies in systems that erode or are dissolute by time (44) (Supplementary Table I), while all stored formulae followed the Higuchi model (Supplementary Table II).

The Absolute Percent Crystallinity

The absolute percent crystallinity data for prepared samples were calculated, and values were presented in Table II. Inverse relationship was observed between absolute percent crystallinity and Q_{10min} and Q_{30min}, where reduction in the crystallinity value was associated with a considerable improvement in Q_{10min} and Q_{30min}. The lowest absolute percent value was observed for the formula in run number 24 (Table II), suggesting greatest amorphousness compared to the other studied samples.

Solubility Studies

The solubility data were studied to reveal potential correlations between the studied factors and the maximum solubility (S_{max}) of MX from PMs and their corresponding SDs (Table II). The MX-S_{max} in distilled water was extremely low about 10.98 ± 0.93 µg/mL at 25°C which is equivalent to MX-S_{max} reported value of 12 µg/ml (61), while the solubility of all prepared samples was improved.

Drug loading % (A) has a negative effect on MX-S_{max} values; increasing drug loading % (A), at a certain level of both carriers' ratio (B) and method of preparation (C), would decrease MX-S_{max} as presented in (Table II).

On the other hand, carriers' ratio (B) exhibited an obvious positive effect on MX-S_{max} values. In other words, at a constant level of other factors, MX-S_{max} would increase by increasing SOL in the ratio of the carriers. This could be ascribed to the high-water solubility of the studied carriers.

Method of preparation (C) clearly influences MX solubility values where MX-S_{max}, at low level of A (-1), increased by about $\approx$ 3-, 4-, and 9-fold for PM, FM and HME, respectively. HME plays a pivotal role on enhancing MX-S_{max} followed by FM and PM.

The result indicated that the combination of the lowest level (-1) of factor A and the highest level (+ 1) of factor B when using a HME technique resulted in the highest MX-S_{max} value. This result complies with the *in vitro* dissolution data.

Multiple Response Optimization

A multiple response optimization approach was conducted to obtain the required optimized characteristics that give the maximum Q_{10min} and Q_{30min} for both fresh and stored samples. To simultaneously optimize four different responses, a multi-criteria decision approach such as numerical optimization by the desirability function was utilized to estimate the optimum settings for the formulation (34). The desirability function of the given responses and factors is the base, on which the numerical optimization tool in the Design-Expert® software is dependent. Desirability is simply a mathematical method to find the optimum configuration of the studied factors (62). The desirability function is an alteration of the response variable from a 0 to 1 scale. The desirability of 0 symbolized a completely undesirable response, while 1 symbolized the most desirable response (63, 64).

The numerical optimization technique was based on maximizing all responses Y_1 (Q_{10min}-fresh), Y_2 (Q_{30min}-fresh), Y_3 (Q_{10min}-stored), and Y_4 (Q_{30min}-stored) to meet the target dissolution stated by FDA: $Q_{30min} \geq 75\%$. In the same section criteria, the independent variables were set within their minimum and maximum ranges.

The design space can be supplemented by set the target responses to meet a rapid dissolution profile ($Q_{30min} \geq 75\%$). The graphical depiction of the overlapping common region of design space for successful formulation ranges is presented in Figure 6, which is represented by the yellow area.

The HME formula containing 2.5% drug loading (A; level −1) and a high ratio of SOL in SOL/POLX (B) of (80-20; level 1) (run number 24) was selected as the optimized system (OPT) with a desirability value of "1" (Figure 6), which manufactured using combination of analyzed factors in the range shown in yellow in the design space. In all studied responses, OPT was the only composition that gave fast dissolution ($Q_{10min} \geq 75\%$) from both fresh and storage samples.

The optimized formula (OPT) was prepared ($n = 3$), and the responses (Y_1–Y_4) were re-assessed to evaluate the reliability of the suggested optimization model. The predicted values by the multilevel factorial design were compared with the experimental results (Table IV). The lower magnitude of % relative errors (0.76%, −0.01%, 3.33%, and −0.06% for Y_1, Y_2, Y_3, and Y_4, respectively) could indicate reasonable agreements and/or no marked differences between the current and previous experimental results. It is evidence of the high extrapolative ability and robustness of the developed optimization model (65, 66). According to the results of the verification phase, OPT was progressed for further characterization studies.

For validation of the model, the calculation of predicted values of the responses for the 27 runs was carried out and was found to be in close agreement with the experimental (actual) values as illustrated in Figure 3. Moreover, the models were validated through proposed checkpoints (3 formulae, X1–X3; $n = 3$) that were not involved in the matrix of the design. Table IV shows that the detected values of responses of these checkpoints were in close agreement with

the predicted values of the model (% relative error = <5%), indicating the validity and practicability of the suggested models (67). The percent relative error was calculated from the following equation (67):

Relative error = (predicted value-experimental value) / (predicted value)   Equation (20)

Characterization of the Optimized Formulation

MX Dissolution Rate and Kinetics

Figure 7 illustrates the MX dissolution profiles of the optimized formula (OPT) from fresh and 3-month storage samples in different pHs. In 0.1N HCL (pH 1.2), MX powder displayed the slowest dissolution rate of 2.8% in 60 min as previously reported (51). A promising improvement in the dissolution of MX was seen with Q_{30min} of 65.27% and 62.51% from both fresh and 3-month stored OPT samples,

respectively. This is assigned to the molecular dispersion of MX in the studied carriers with improved wettability.

Comparable dissolution profiles were observed with Q_{30min} of 99.73% and 96.99% from fresh and 97.01% and 94.35% from 3-month storage OPT samples in pH 7.4 and distilled water, respectively (Figure 7). These results fulfilled the acceptance criterion in the USP and the requirement for an IR dosage form (Q ≥ 75% in 30 min) as well as demonstrated good stability characteristics for 3-month storage under stress conditions (f_2= 81). The enhancement of MX dissolution rate was attributed to engaging the effects of the studied drug loading % (A, significant negative effect) and the studied carriers' ratio (B, significant positive effect) using the HME technique. In other words, HME resulted in the formation of a glassy solution in which the drug was dispersed molecularly in the carriers' matrix with improved wettability (68).
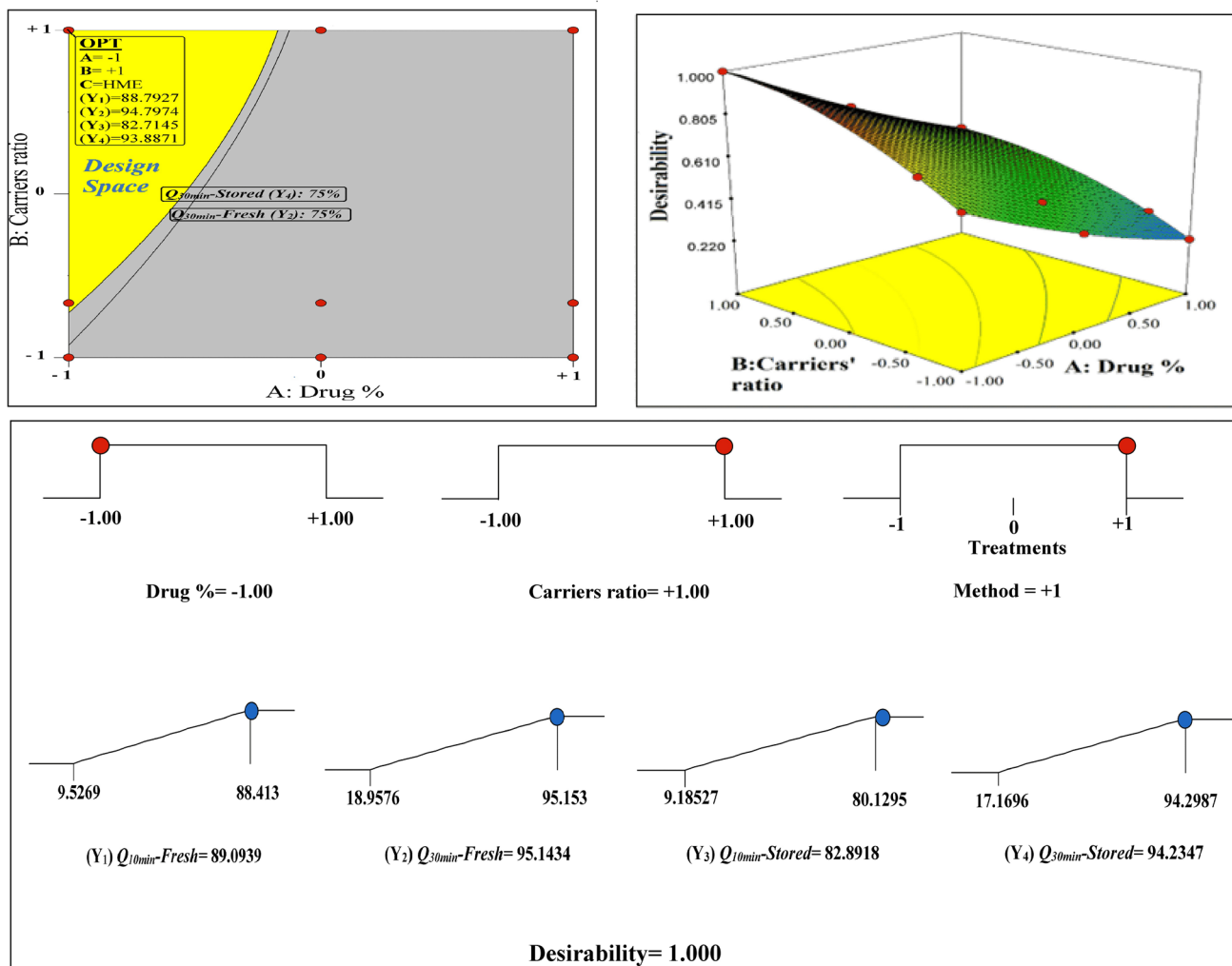

Fig. 6 Design space and desirability 3-D plot and ramps for the optimized formula (OPT)

Table IV Model Validation by Comparing the Predicted Values with the Observed Experimental Values

Check points	Independent variables			Dependent variables (responses)									
	A	B	C	Y1			Y2			Y3			Y4		
	(Drug loading %)	(Mixed carriers' ratio)	(Method of preparation)	Predicted value (%)	Experimental value	Percent relative error (%)	Predicted value (%)	Experimental value	Percent relative error (%)	Predicted value (%)	Experimental value	Percent relative error (%)	Predicted value (%)	Experimental value	Percent relative error (%)
X1	2.55	1.29	PM	17	16.80±1.96	1.18	24.9	25.25±1.13	−1.57	15.5	15.26±0.89	1.55	24	23.59±1.20	1.53
X2	3.84	3.43	PM	25.7	25.92±2.06	−0.94	29.7	29.37±1.54	1.08	23.5	23.80±1.88	−1.36	28.7	28.31±1.13	1.46
X3	2.52	1	HME	55.6	56.03±1.75	−0.79	74.1	75.13±2.30	−1.43	50.2	51.04±2.21	−1.67	70.6	69.77±0.96	1.17
OPT	2.5	4	HME	89.1	88.41±1.15	0.76	95.1	95.15±1.31	−0.01	82.9	80.13±1.68	3.33	94.2	94.30±1.27	−0.06

The experimental data is given as the mean ± SD (n = 3)

It is worthy to mention that the dissolution profile of pure MX powder and the market product (Mobic®, 15 mg) in distilled water was previously studied and both products exhibited very slow dissolution rates (4.90% and 51.71% in 30 min, respectively) (51). Accordingly, the optimized formula would guarantee an immediate release pattern with a faster onset of MX dissolution. The mechanism of MX dissolution from the optimized formula (OPT) in distilled water followed the Higuchi square root of the time-release kinetics model before and after storage based on the highest regression coefficient (r^2).

DSC Thermogram

Figure 8 shows DSC thermograms of pure MX, SOL, POLX, the optimized formula (OPT), and its stored sample. DSC thermogram of pure MX was characterized by a sharp endothermic peak at 260.87°C (ΔH= 56.24 J/g), corresponding to the melting point (69). SOL is an amorphous copolymer with a glass transition temperature (Tg) value of 71.52°C (70), whereas POLX melting endotherm was detected at 58.59°C (71).

DSC thermogram of the optimized formula (OPT) showed almost disappearance of the characteristic MX endothermic peak with subsequent reduction in ΔH-value (Figure 8). This could be explained by the dispersion of the drug in the molten carrier(s), the formation of a glassy solution, and/or the gradual conversion to an amorphous form (72). The calculated absolute percent crystallinity for the freshly prepared OPT and the 3-month stored sample was 13.42% and 15.21%, respectively, revealing the high stability of the OPT formula even under stress conditions for 3 months.

X-Ray Diffraction (XRD)

Figure 8 shows XRD patterns of MX, SOL, POLX, the optimized formula (OPT), and its stored sample. MX is a crystalline drug, as previously reported in the literature (73), and reveals characteristic high-intensity diffraction fingerprints at 13.09°, 14.97°, 18.65°, and 25.99° (2θ). However, flat pattern peaks with very low intensities were detected which is characteristic of amorphous SOL(74). Sharp peaks on the POLX diffractogram at (2θ) values of 19.21° and 23.74° with a significant broad halo were detectable which is a typical distinctive property of POLX structure with crystalline domains set in the amorphous regions (75).

The diffraction patterns of the OPT and its stored sample showed a clear reduction in the intensity of all MX discriminatory peaks (Figure 8); the drug might be dissolved in the carriers' matrix in an amorphous state as observed in the DSC studies.
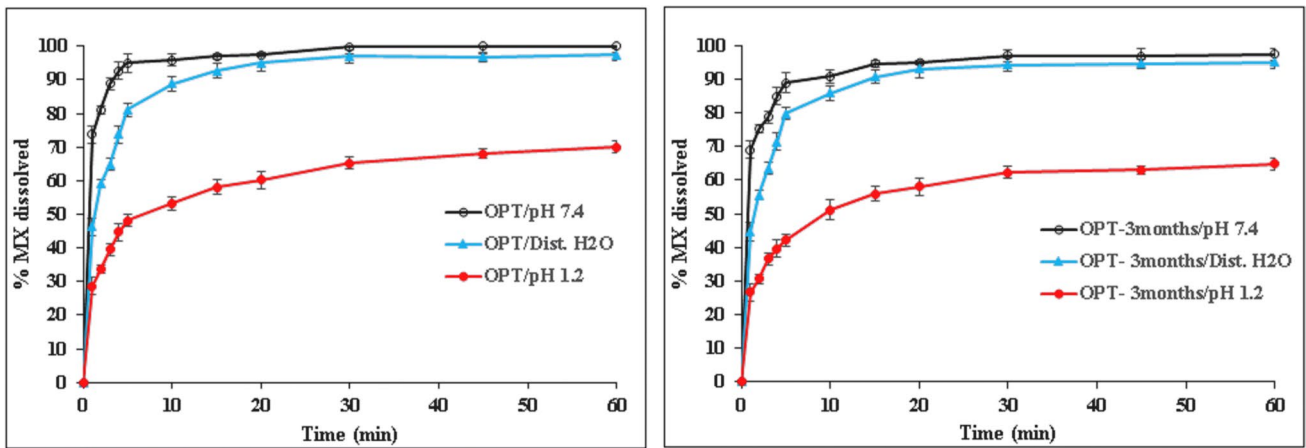
Fig. 7 Dissolution profile of MX the optimized formula (OPT) from fresh and 3-month storage samples in different pHs
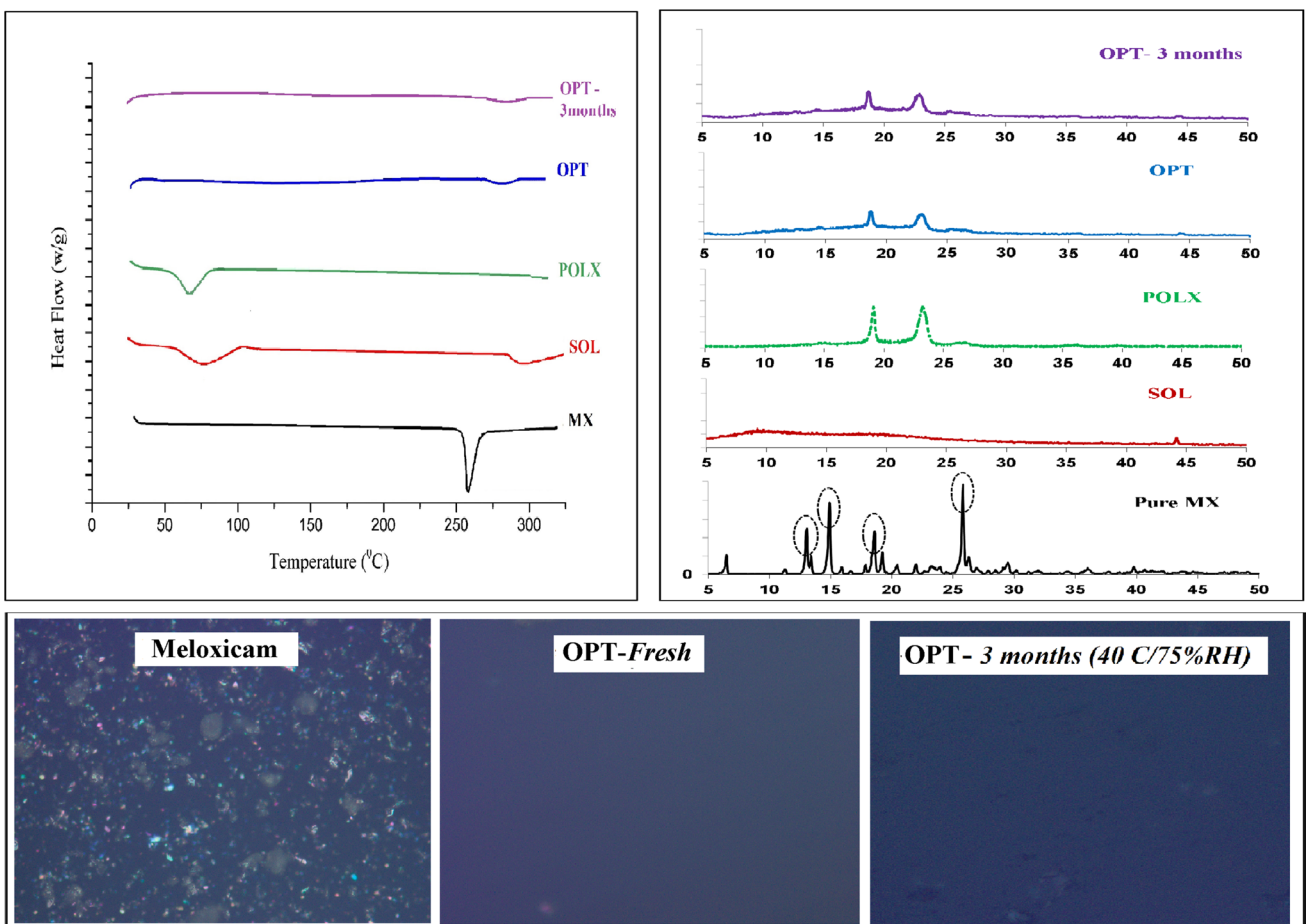

Fig. 8 DSC thermograms, XRD patterns, and PLM observations of pure MX, SOL, POLX, the optimized formula (OPT), and its corresponding stored sample.

PLM Imaging of the Optimized Formulation

Figure 8 shows morphological observation of MX and the optimized formula (OPT) utilizing PLM. Crystalline MX powder clearly showed intense birefringence, while no or trace birefringence was detected for the optimized MX formula, which confirmed MX amorphous state.

Conclusion

For the first time, successful application of 3^3 full factorial design of RSM in the optimization of formulations of MX/SDs, for studying the dissolution enhancement of MX/SDs. This allowed the understanding of the outcome of factors' interaction and prediction of responses, showing how these factors can affect MX dissolution before and after storage. The design showed a good prediction capability after validation. The derived polynomial equations and 3-D response surface plots aid in predicting the values of the selected independent variables which can achieve the optimum dissolution profiles. The optimized formulation prepared by the HME technique using a novel combination of carriers SOL:POLX (80:20), as per the optimization design, successfully succeeded to give a stable and fast dissolution profile.

Declarations

Conflict of Interest The authors declare no competing interests.

REFERENCES

1. Tran P, Pyo Y-C, Kim D-H, Lee S-E, Kim J-K, Park J-S. Overview of the manufacturing methods of solid dispersion technology for improving the solubility of poorly water-soluble drugs and application to anticancer drugs. J Pharmaceutics. 2019;11:132. https://doi.org/10.3390/pharmaceutics11030132.
2. Vasconcelos T, Marques S, das Neves J, Sarmento B. Amorphous solid dispersions: rational selection of a manufacturing process. Adv Drug Deliv Rev. 2016;100:85–101. https://doi.org/10.1016/j.addr.2016.01.012.
3. Janssens S, Van den Mooter G. Review: physical chemistry of solid dispersions. J Pharm Pharmacol. 2009;61:1571–86. https://doi.org/10.1211/jpp.61.12.0001.
4. Lenz E, Löbmann K, Rades T, Knop K, Kleinebudde P. Hot melt extrusion and spray drying of co-amorphous indomethacin-arginine with polymers. J Pharm Sci. 2017;106:302–12. https://doi.org/10.1016/j.xphs.2016.09.027.
5. Smeets A, Koekoekx R, Clasen C, Van den Mooter G. Amorphous solid dispersions of darunavir: comparison between spray drying and electrospraying. Eur J Pharm Biopharm. 2018;130:96–107. https://doi.org/10.1016/j.ejpb.2018.06.021.
6. Choi J-S, Lee S-E, Jang WS, Byeon JC, Park J-S. Solid dispersion of dutasteride using the solvent evaporation method: approaches to improve dissolution rate and oral bioavailability in rats. Mater Sci Eng C. 2018;90:387–96. https://doi.org/10.1016/j.msec.2018.04.074.
7. UmakantVerma J, Mokale V. Preparation of freeze-dried solid dispersion powder using mannitol to enhance solubility of lovastatin and development of sustained release tablet dosage form. Am J Pharma Sci Nanotechnol. 2014;1:11–26.
8. Zhao Y, Xie X, Zhao Y, Gao Y, Cai C, Zhang Q, et al. Effect of plasticizers on manufacturing ritonavir/copovidone solid dispersions via hot-melt extrusion: Preformulation, physicochemical characterization, and pharmacokinetics in rats. Eur J Pharm Sci. 2019;127:60–70.
9. Genina N, Hadi B, Löbmann K. Hot melt extrusion as solvent-free technique for a continuous manufacturing of drug-loaded mesoporous silica. J Pharm Sci. 2018;107:149–55.
10. Emara LH, Abdelfattah FM, Taha NF, El-Ashmawy AA, Mursi NM. In vitro evaluation of ibuprofen hot-melt extruded pellets employing different designs of the flow through cell. J Int J Pharm Pharm Sci. 2014;6.
11. Emam MF, Taha NF, Emara LH. A novel combination of Soluplus® / poloxamer for meloxicam solid dispersions via hot melt extrusion for rapid onset of action. Part 1: Dissolution and stability studies. J Appl Pharm Sci. 2021.
12. Simões MF, Pinto RM, Simões S. Hot-melt extrusion in the pharmaceutical industry: toward filing a new drug application. Drug Discov Today. 2019. https://doi.org/10.1016/j.drudis.2019.05.013.
13. Emara LH, Abdelfattah FM, Taha NF. Hot melt extrusion method for preparation of ibuprofen/sucroester WE15 solid dispersions: evaluation and stability assessment. J Appl Pharm Sci. 2017;7:156–67.
14. Djuris J, Nikolakakis I, Ibric S, Djuric Z, Kachrimanis K. Preparation of carbamazepine–Soluplus® solid dispersions by hot-melt extrusion, and prediction of drug–polymer miscibility by thermodynamic model fitting. Eur J Pharm Biopharm. 2013;84:228–37. https://doi.org/10.1016/j.ejpb.2012.12.018.
15. Patil H, Tiwari RV, Repka MA. Hot-melt extrusion: from theory to application in pharmaceutical formulation. AAPS Pharmscitech. 2016;17:20–42.
16. Chokshi RJ, Sandhu HK, Iyer RM, Shah NH, Malick AW, Zia H. Characterization of physico-mechanical properties of

indomethacin and polymers to assess their suitability for hot-melt extrusion processs as a means to manufacture solid dispersion/solution. J Pharm Sci. 2005;94:2463–74.

17. Hoashi Y, Tozuka Y, Takeuchi H. Completely dry process for the desired release profile of poorly water-soluble drugs by a temperature-controllable twin-screw kneader. Asian J Pharm Sci. 2011;6:101–8.

18. DiNunzio JC, Brough C, Hughey JR, Miller DA, Williams RO III, McGinity JW. Fusion production of solid dispersions containing a heat-sensitive active ingredient by hot melt extrusion and Kinetisol® dispersing. Eur J Pharm Biopharm. 2010;74:340–51.

19. Hughey JR, DiNunzio JC, Bennett RC, Brough C, Miller DA, Ma H, et al. Dissolution enhancement of a drug exhibiting thermal and acidic decomposition characteristics by fusion processing: a comparative study of hot melt extrusion and KinetiSol® dispersing. AAPS Pharmscitech. 2010;11:760–74.

20. Wilson MR, Jones DS, Andrews GP. The development of sustained release drug delivery platforms using melt-extruded cellulose-based polymer blends. J Pharm Pharmacol. 2017;69:32–42.

21. Thiry J, Krier F, Evrard B. A review of pharmaceutical extrusion: critical process parameters and scaling-up. Int J Pharm. 2015;479:227–40.

22. Ditzinger F, Dejoie C, Sisak Jung D, Kuentz M. Polyelectrolytes in hot melt extrusion: a combined solvent-based and interacting additive technique for solid dispersions. J Pharmaceutics. 2019;11:174.

23. Vijaya Kumar SG, Mishra DN. Preparation and evaluation of solid dispersion of meloxicam with skimmed milk. Yakugaku Zasshi. 2006;126:93–7.

24. Kumar SGV, Mishra DN. Preparation, characterization and in vitro dissolution studies of solid dispersion of Meloxicam with PEG 6000. Yakugaku Zasshi. 2006;126:657–64.

25. Ghareeb MM, Abdulrasool AA, Hussein AA, Noordin MI. Kneading technique for preparation of binary solid dispersion of meloxicam with poloxamer 188. AAPS Pharmscitech. 2009;10:1206–15.

26. Haser A, Huang S, Listro T, White D, Zhang F. An approach for chemical stability during melt extrusion of a drug substance with a high melting point. Int J Pharm. 2017;524:55–64. https://doi.org/10.1016/j.ijpharm.2017.03.070.

27. Haser A, Cao T, Lubach JW, Zhang F. In situ salt formation during melt extrusion for improved chemical stability and dissolution performance of a meloxicam–copovidone amorphous solid dispersion. Mol Pharm. 2018;15:1226–37. https://doi.org/10.1021/acs.molpharmaceut.7b01057.

28. Emara LH, Emam MF, Taha NF, El-ashmawy AAE-R, Mursi NM. In-vitro dissolution study of meloxicam immediate release products using flow through cell (Usp Apparatus 4) under different operational conditions. Int. J Pharm Pharm Sci. 2014;6 https://www.researchgate.net/publication/269222632.

29. Suzuki H, Yakushiji K, Matsunaga S, Yamauchi Y, Seto Y, Sato H, et al. Amorphous solid dispersion of meloxicam enhanced oral absorption in rats with impaired gastric motility. J Pharm Sci. 2018;107:446–52.

30. Türck D, Roth W, Busch U. A review of the clinical pharmacokinetics of meloxicam. Rheumatology. 1996;35:13–6. https://doi.org/10.1093/rheumatology/35.suppl_1.13/JRheumatology.

31. Reintjes T. Solubility enhancement with BASF pharma polymers: Solubilizer compendium 2011.

32. Hughey JR, Keen JM, Brough C, Saeger S, McGinity JW. Thermal processing of a poorly water-soluble drug substance exhibiting a high melting point: the utility of KinetiSol® dispersing. Int J Pharm. 2011;419:222–30. https://doi.org/10.1016/j.ijpharm.2011.08.007.

33. Taha NF, Emam MF, Emara LH. A novel combination of Soluplus®/poloxamer for meloxicam solid dispersions via hot melt extrusion for rapid onset of action. Part 2:

comparative bioavailability and IVIVC. Drug Dev Indust Pharm. 2020;46:1362–72. https://doi.org/10.1080/03639045.2020.1791164.

34. Myers RH, Montgomery DC, Anderson-Cook CM. Response surface methodology: process and product optimization using designed experiments. 3rd ed. ed: John Wiley & Sons, Inc.; 2009.

35. Bezerra MA, Santelli RE, Oliveira EP, Villar LS, Escaleira LA. Response surface methodology (RSM) as a tool for optimization in analytical chemistry. Talanta. 2008;76:965–77.

36. Teofilo R, Ferreira M. Chemometrics II: electronic spreadsheets for the calculation of experimental design, a tutorial. Quim Nova. 2006;29:338–50.

37. Rajasimman M, Sangeetha R. Optimization of process parameters for the extraction of chromium (VI) by emulsion liquid membrane using response surface methodology. J Hazard Mater. 2009;168:291–7.

38. Rakić T, Kasagić-Vujanović I, Jovanović M, Jančić-Stojanović B, Ivanović D. Comparison of full factorial design, central composite design, and Box-Behnken design in chromatographic method development for the determination of fluconazole and its impurities. Anal Lett. 2014;47:1334–47.

39. Emara LH, Emam MF, Taha NF, Raslan HM, El-Ashmawy AA. A simple and sensitive HPLC/UV method for determination of meloxicam in human plasma for bioavailability and bioequivalence studies. J Appl Pharm Sci. 2016;6:012–9. https://doi.org/10.7324/JAPS.2016.60702.

40. Philip AK, Pathak K. Osmotic flow through asymmetric membrane: a means for controlled delivery of drugs with varying solubility. AAPS Pharmscitech. 2006;7:E1–E11.

41. Sood A, Panchagnula R. Drug release evaluation of diltiazem CR preparations. Int J Pharm. 1998;175:95–107.

42. Karasulu E, Yesim Karasulu H, Ertan G, Kirilmaz L, Guneri T. Extended release lipophilic indomethacin microspheres: formulation factors and mathematical equations fitted drug release rates. Eur J Pharm Sci. 2003;19:99–104.

43. Wright MR. The kinetic analysis of experimental data. An introduction to chemical kinetics: Wiley, J., and Sons Ltd., The Atrium, Southern Gate, Chichester, West Suessex PO19 8SQ, England; 2004. p. 43-95.

44. Hixson A, Crowell J. Dependence of reaction velocity upon surface and agitation. Ind Eng Chem Res. 1931;23:923–31.

45. Higuchi TJAACI. A phase solubility technique, vol. 4; 1965. p. 117–211.

46. Moore JW, Flanner HH. Mathematical comparison of dissolution profiles. Pharm Technol. 1996;20:64–74 http://pascal-francis.inist.fr/vibad/index.php?action=getRecordDetail&idt=3112822.

47. U.S. FDA. Dissolution testing of immediate release solid oral dosage forms; guidance for industry;. 1997.

48. Bhattachar SN, Wesley JA, Fioritto A, Martin PJ, Babu SR. Dissolution testing of a poorly soluble compound using the flow-through cell dissolution apparatus. Int J Pharm. 2002;236:135–43.

49. Emam MF. Improvement of the dissolution and bioavailability of a non-steroidal anti-inflammatory drug. Cairo University; 2015.

50. Taha NF, Emam MF, Emara LH. A novel combination of Soluplus®/poloxamer for meloxicam solid dispersions via hot melt extrusion for rapid onset of action. Part 2: comparative bioavailability and IVIVC. J Drug Dev Ind Pharm. 2020;46:1362–72.

51. Emam MF, Taha NF, Emara LH, Mursi NM. Preparation, characterization and in-vitro / in-vivo evaluation of meloxicam extruded pellets with enhanced bioavailability and stability. J Drug Dev Ind Pharm. 2021;47:163–75.

52. Elsayed EW, El-Ashmawy AA, Mursi NM, Emara LH. Optimization of gliclazide loaded alginate-gelatin beads employing central composite design. Drug development and industrial pharmacy. 2019;45:1959–72.

53. Gu B, Linehan B, Tseng Y-C. Optimization of the Büchi B-90 spray drying process using central composite design for preparation of solid dispersions. Int J Pharm. 2015;491:208–17.

54. Ahmadkhaniha D, Heydarzadeh Sohi M, Zarei-Hanzaki A, Bayazid SM, Saba M. Taguchi optimization of process parameters in friction stir processing of pure Mg. Journal of Magnesium and Alloys. 2015;3:168–72. https://doi.org/10.1016/j.jma.2015.04.002.

55. Taheri M, Bagheri M, Moazeni-Pourasil RS, Ghassempour A. Response surface methodology based on central composite design accompanied by multivariate curve resolution to model gradient hydrophilic interaction liquid chromatography: Prediction of separation for five major opium alkaloids. Journal of separation science. 2017;40:3602–11.

56. BritishPharmacopoeia. British Pharmacopoeia Commission, London: The Stationary Office.; 2007.

57. Food U, Administration D. Guidance for industry SUPAC-MR: Modified release solid oral dosage forms scale-up and postapproval changes: chemistry, manufacturing. and controls. 1997.

58. USP29-NF24 UP. USP Monographs: Meloxicam Tablets. 2011.

59. Vasoya JM, Desai HH, Gumaste SG, Tillotson J, Kelemen D, Dalrymple DM, et al. Development of solid dispersion by hot melt extrusion using mixtures of polyoxylglycerides with polymers as carriers for increasing dissolution rate of a poorly soluble drug model. J Pharma Sci. 2019;108:888–96.

60. Pina MF, Zhao M, Pinto JF, Sousa JJ, Craig DQ. The influence of drug physical state on the dissolution enhancement of solid dispersions prepared via hot-melt extrusion: a case study using olanzapine. J Pharma Sci. 2014;103:1214–23.

61. Seedher N, Bhatia S. Solubility enhancement of Cox-2 inhibitors using various solvent systems. Aaps Pharm Sci Tech. 2003;4:36–44.

62. Raja RS, Manisekar K. Experimental and statistical analysis on mechanical properties of nano flyash impregnated GFRP composites using central composite design method. Mat Design. 2016;89:884–92.

63. Mundada PK, Sawant KK, Mundada VP. Formulation and optimization of controlled release powder for reconstitution for metoprolol succinate multi unit particulate formulation using risk based QbD approach. J Drug Deliv Sci Technol. 2017;41:462–74.

64. Harrington EC. The desirability function. Industrial quality control. 1965;21:494-498.

65. Das SK, Khanam J, Nanda A. Optimization of preparation method for ketoprofen-loaded microspheres consisting polymeric blends using simplex lattice mixture design. J Mater Sci Eng C. 2016;69:598–608.

66. Dhat S, Pund S, Kokare C, Sharma P, Shrivastava B. Risk management and statistical multivariate analysis approach for design and optimization of satranidazole nanoparticles. Euro J Pharm Sci. 2017;96:273–83.

67. Sankalia MG, Mashru RC, Sankalia JM, Sutariya VB. Reversed chitosan–alginate polyelectrolyte complex for stability improvement of alpha-amylase: optimization and physicochemical characterization. Eur J Pharm Biopharm. 2007;65:215–32.

68. Zhang Y, Liu Y, Luo Y, Yao Q, Zhong Y, Tian B, et al. Extruded Soluplus/SIM as an oral delivery system: characterization, interactions, in vitro and in vivo evaluations. Drug Deliv. 2016;23:1902–11. https://doi.org/10.3109/10717544.2014.960982.

69. Etman M, Shekedef M, Nada A, Ismail A. In vitro and in vivo evaluation of tablets containing meloxicam-PEG 6000 ball-milled co-ground mixture. J Appl Pharm Sci. 2017;7:031–9. https://doi.org/10.7324/japs.2017.70306.

70. Gupta SS, Meena A, Parikh T, Serajuddin AT. Investigation of thermal and viscoelastic properties of polymers relevant to hot melt extrusion-I: polyvinylpyrrolidone and related polymers. J Ex Food Chem. 2016;5:1001 https://ojs.abo.fi/ojs/index.php/jefc/article/view/344.

71. Swain RP, Subudhi BB. Effect of semicrystalline copolymers in solid dispersions of pioglitazone hydrochloride: in vitro-in vivo correlation. Drug Dev Ind Pharm. 2019;45:775–86. https://doi.org/10.1080/03639045.2019.

72. Newa M, Bhandari KH, Li DX, Kwon T-H, Kim JA, Yoo BK, et al. Preparation, characterization and in vivo evaluation of ibuprofen binary solid dispersions with poloxamer 188. Int J Pharm. 2007;343:228–37. https://doi.org/10.1016/j.ijpharm.2007.05.031.

73. Sharma S, Sher P, Badve S, Pawar APJAP. Adsorption of meloxicam on porous calcium silicate: characterization and tablet formulation. 2005;6:E618-EE25.

74. Hughey JR, Keen JM, Miller DA, Kolter K, Langley N, McGinity JWJEJoPS. The use of inorganic salts to improve the dissolution characteristics of tablets containing Soluplus®-based solid dispersions. 2013;48:758-766.

75. Ali W, Williams AC, Rawlinson CF. Stochiometrically governed molecular interactions in drug: poloxamer solid dispersions. Int J Pharm. 2010;391:162–8. https://doi.org/10.1016/j.ijpharm.2010.03.014.